IEEE Photonics Journal
An IEEE Photonics Society Publication

Open Access

Ultrahigh Temperature Sensitivity Using Photonic Bandgap Effect in Liquid-Filled Photonic Crystal Fibers

Volume 9, Number 3, June 2017

Lan Cheng
Jian-jun Wu
Xiong-wei Hu
Jing-gang Peng
Lu-yun Yang
Neng-li Dai
Jin-yan Li

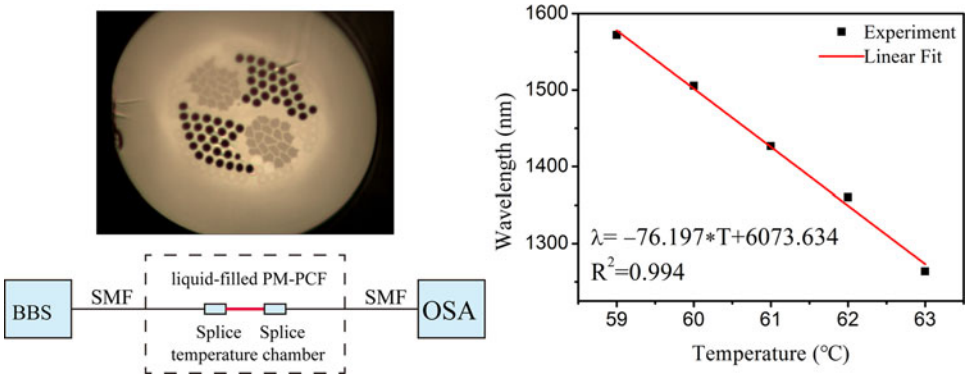

DOI: 10.1109/JPHOT.2017.2700291
1943-0655 © 2017 IEEE

Ultrahigh Temperature Sensitivity Using Photonic Bandgap Effect in Liquid-Filled Photonic Crystal Fibers

Lan Cheng, Jian-jun Wu, Xiong-wei Hu, Jing-gang Peng, Lu-yun Yang, Neng-li Dai, and Jin-yan Li

Wuhan National Laboratory of Optoelectronics, Huazhong University of Science and Technology, Wuhan 430074, China

DOI:10.1109/JPHOT.2017.2700291

Manuscript received March 9, 2017; revised April 12, 2017; accepted April 27, 2017. Date of publication May 16, 2017; date of current version May 31, 2017. This work was supported by the Natural National Science Foundation of China under Grant 61535009. Corresponding author: Jin-yan Li (e-mail: ljy@mail.hust.edu.cn).

Abstract: We theoretically and experimentally investigate the temperature responses of two liquid-filled polarization maintaining photonic crystal fibers (PM-PCFs). The guidance mechanism of liquid-filled PM-PCFs is a hybrid of the modified total internal reflection and photonic bandgap (PBG) principles. According to the wavelength shifting of photonic band edges, a sensitivity of −10.033 nm/°C from 38 °C to 45 °C was achieved in the glycerol-filled PM-PCF, whereas an ultrahigh sensitivity up to –76.197 nm/°C from 59 °C to 63 °C was obtained in the toluene-filled PM-PCF. High temperature sensitivities stem from the high transmission window located in the first PBG. The thermal tunable filled PCFs with PBG effect properties will offer great potential for temperature sensing, as well as tunable bandpass filters.

Index Terms: Photonic crystal fiber (PCF), temperature sensor, fluid.

1. Introduction

Due to the special structures and optical properties, photonic crystal fibers (PCFs) have attracted great attention over the past few decades [1], [2]. PCFs are divided into modified total internal reflection (MTIR) and photonic bandgap (PBG) fibers by the guidance mechanism [1], [2]. A variety of functional materials can be filled into the air holes of PCFs, providing a promising candidate for developing communication and sensing applications, such as tunable filters [3], optical switches [4], and attenuators [5]. The favorite filled materials reported in literatures are liquid crystals [6]–[8], magnetic fluid [9], [10], refractive index matching liquid [11]–[13], etc. The thermo-optic coefficient of liquid is generally two orders of magnitude higher than that of silica; therefore, filling liquid into the air holes of PCF can significantly improve the temperature sensitivity [14]. For example, an average temperature sensitivity of ∼54.3 nm/°C from 34.0 °C to 35.4 °C was obtained by filling standard 1.46 refractive index liquid into one air hole of PCF [15]. The means of filling a high index material into the air holes can convert a MTIR PCF to a PBG fiber. Thus the wavelength of photonic band edges (PBEs) shifts greatly with changes of temperature, offering a method to achieve temperature measurement except for modal interference. Based on the bandgap-like effect, a temperature sensitivity up to −5.5 nm/°C was experimentally validated in a selectively liquid-filled PCF [16]. By arranging the air holes and high index rods in a radial [17], [18] or linear way [19],

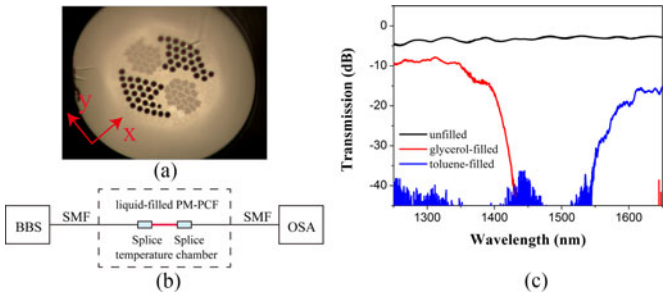

Fig. 1. (a) Optical micrograph of PM-PCF ends face. (b) Schematic diagram of the experimental setup. (c) Transmission spectrum of unfilled PM-PCF and filled PM-PCFs at 27 °C.

some research groups have fabricated hybrid PCFs, which behaves the properties of both MTIR and PBG structures. In a hybrid PCF by selective-filling, a temperature sensitivity of −45.8 nm/°C at 56.5 °C was achieved based Sagnac interferometers [20].

In this paper, we fabricated two hybrid PCFs based on the liquid-filled polarization maintaining photonic crystal fibers (PM-PCFs), whose temperature responses were investigated both theoretically and experimentally. High temperature sensitivities were achieved based on the wavelength shifting of PBEs. The mechanisms for high temperature sensitivities were also discussed. These kinds of filled PCFs could be used to develop all-fiber optical filters and sensors.

2. Fiber Fabrication and Experiment Setup

Fig. 1(a) shows the optical microscope image of the PM-PCF, which was made by the standard stack-and-draw process. The fiber diameter and core diameter are 115 um and 9.2 um, respectively. Two fan-shaped areas at x-axis have an air hole pitch (Λ) of 5.0 um and a 66% ratio (d/Λ) of hole diameter to pitch. Two other fan-shaped areas at y-axis are formed by replacing air holes with boron-doped rods. The filled PM-PCFs were prepared as follows: firstly, stripping the fiber coating of both end, cleaning and cutting the fiber ends; then, one end of the fiber was inserted to the needle of injection syringe and fixed with a super glue; at last, adding pure glycerol or toluene into the injection syringe and fixing the syringe on a pressure equipment made by ourselves, increasing the pressure of injection syringe with a precession nut to fill the fiber with liquids efficiently.

Fig. 1(b) shows the experimental setup of temperature measurement. A broadband source (BBS, 1250–1650 nm) was employed as the incident light source and the emitted light was monitored by an optical spectrum analyzer (OSA, YOKOGAWA AQ6370D). Both ends of the filled PM-PCFs were spliced to a standard single mode fiber (SMF). The filled PM-PCFs were placed in a temperature chamber with an accuracy of 0.1 °C to endure different temperatures. To obtain a precise temperature control, the temperature chamber was heated to the highest temperature (100 °C) that the temperature chamber can bear, and then natural cooled. Natural cooling can lead to a slowly decreasing temperature around the filled PM-PCFs. During the experiments, the filled PM-PCFs were kept straight in the temperature chamber to prevent bending and torsion. The experiment fiber lengths are 19.2 cm for glycerol-filled PM-PCF and 7.8 cm for toluene-filled PM-PCF, respectively.

The transmission spectrums of unfilled PM-PCF (the fiber length is 8 cm) and two filled PM-PCFs at room temperature (27 °C) were shown in Fig. 1(c). Because of almost the same size of mode field area with the SMF, the PM-PCF has low splicing loss of about 3 dB. The guidance mechanism of unfilled PM-PCF is MTIR due to the lower refractive indices of both boron-doped rods and air holes than that of silica. The high transmission window was observed in the short wavelength direction for the glycerol-filled PM-PCF, whereas in the long wavelength direction for the toluene-filled PM-PCF. Owing to the higher refractive indexes of glycerol and toluene than that of silica, the guidance mechanism shift to the PBG effect along the filling direction (x-axis), which gives rise to the high transmission window of filled PM-PCFs. In the boron-doped direction (y-axis),

the guidance mechanism is still the MTIR. The hybrid PCFs have lower power loss than that of the corresponding PBG fiber, whereas their wavelength filtering property is remained by the PBG effect [20].

3. Theoretical Analysis and Numerical Simulation

The spectral properties of PBG fibers can be described by the anti-resonant reflecting optical waveguide (ARROW) model [21]. Therefore, the locations of transmission minima are positioned at the modal cutoff wavelengths of high-index filler, which can be expressed as

$$\lambda_m = \frac{2d\sqrt{n_2^2 - n_1^2}}{m + 1/2} \tag{1}$$

where m = 1, 2, ..., d is the diameter of individual high-index filler, and n_1 and n_2 are the refractive indices of background material and high-index filler, respectively. For the filled liquid, n_2 is approximately assumed as a linear function of temperature (T, °C)

$$n_2(T) = n_0 + \frac{dn}{dT}(T - T_0) \tag{2}$$

where n_0 is the refractive index at the temperature of T_0, dn/dT is the thermo-optic coefficient. For the glycerol and toluene, the values of n_0 are 1.4746 and 1.4967 (20 °C, 589.3 nm) and the values of dn/dT are $-2.3 \times 10^{-4}\,^{o}C^{-1}$ and $-5.273 \times 10^{-4}\,^{o}C^{-1}$, respectively [22], [23]. Neglecting the thermal-expansion of d, the thermo-optic coefficients of background material silica, and the dispersion of background material silica and high-index filler, the temperature sensitivity of can be expressed

$$\frac{d\lambda_m}{dT} = \frac{4d}{2m + 1} * \frac{n_2}{\sqrt{{n_2}^2 - {n_1}^2}} * \frac{dn_2}{dT}. \tag{3}$$

Due to the negative thermo-optic coefficient of glycerol and toluene, corresponding to the negative values of $d\lambda_m/dT$, the PBEs will be blue-shifted with temperature increasing. The wavelength of PBEs changes faster with temperature for a smaller m value, which means the low order PBG has higher temperature sensitivity than that of high order PBG. The high thermo-optic coefficient also amplifies the temperature sensitivity of PBEs ($d\lambda_m/dT$). The middle term ($n_2/\sqrt{{n_2}^2 - {n_1}^2}$) is a monotonous increasing function of temperature (T), which means the absolute value of $d\lambda_m/dT$ increases with T.

According to the calculated results of bandgap by the plane wave method, the high transmission windows are both located in the first PBG for the two liquid-filledPM-PCFs. In order to investigate the thermal tunable features of two filled PM-PCFs, the bandgap edges of first three PBGs at 27 °C, 32 °C and 37 °C are calculated (see Fig. 2). The intersections of bandgap edges and silica line (1.457) determine the transmission window locations of filled PM-PCFs. Compared with the glycerol-filled PM-PCF, the locations of PBGs shift to longer wavelengths for the toluene-filled PM-PCF and the temperature responses are more significant because of the high thermo-opticcoefficient of toluene. The bandgap properties are similar for two filled PM-PCFs: i) Both the upper and lower edges of three PBG have a blue shift with increasing temperature; ii) the upper edges of each PBG present higher sensitivities to temperature than the lower edges of each PBG, which means a higher sensitivities of the long wavelength edges than the short wavelength edges of PBG; and iii) the low order PBGs shift much faster than high order PBGs. The calculated results are in accordance with the theoretical analysis as above.

4. Experimental Results and Discussions

Firstly, we studied the temperature responses of glycerol-filled PM-PCF. The variation of measured transmission spectra of the glycerol-filled PM-PCF with temperature was shown in Fig. 3(a). The

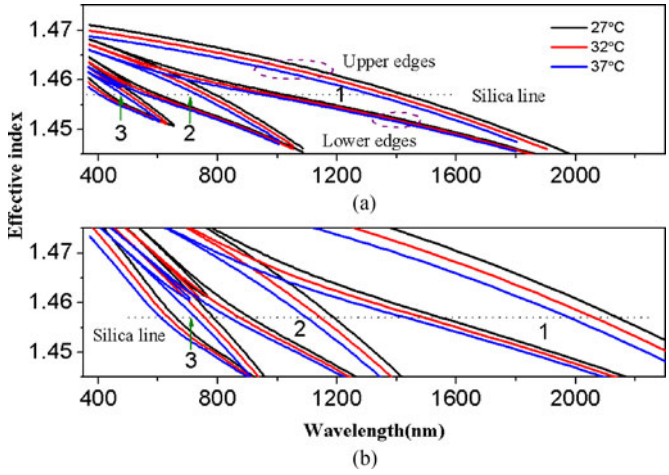

Fig. 2. Calculated bandgap edges at different temperatures in (a) the glycerol-filled and (b) the toluene-filled PM-PCF.

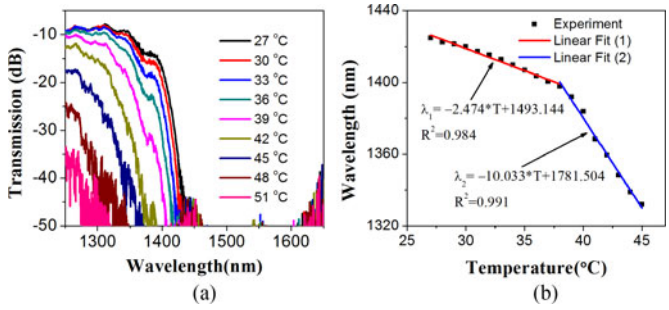

Fig. 3. (a) Transmission spectra at temperature from 27 °C to 51 °C. (b) Correlation between the wavelength of PBEs and temperature for the glycerol-filled PM-PCF.

high transmission window shifts to a shorter wavelength with temperature increasing. There are fluctuations in the spectra for the modal interference. At temperatures above 51 °C, the PBEs shifted out of the spectrum range of BBS. The wavelengths of PBEs at different temperatures were extracted to quantitatively illustrate the wavelength shift of PBEs (Fig. 3(b)). Without loss of generality, the wavelengths corresponding to −35 dB were selected from the data. The relationship between temperature and wavelength of PBEs was obtained by the piecewise linear fitting to intuitively obtain the temperature sensitivity. The high R^2 values mean an excellent goodness-of-fit between the wavelength of PBEs and temperature, and the slopes of fitting curves correspond to the temperature sensitivities. The temperature sensitivities are −2.474 nm/°C from 27 °C to 38 °C and −10.033 nm/°C from 38 °C to 45 °C, respectively. The later one is almost twice of that of a selectively liquid-filled PCF (−5.5 nm/°C) [16]. According to the previous analysis, the high temperature sensitivity is resulted from the high transmission window locating in the first PBG of glycerol-filled PM-PCF.

Owing to the different thermo-optic characteristics of glycerol and toluene, we subsequently tested the temperature responses of toluene-filled PM-PCF, as illustrated in Fig. 4. Compared with the glycerol-filled PM-PCF, the thermally-induced shifts of PBG are obviously accelerated in the toluene-filled PM-PCF. Limited by the spectrum range of BBS, the transmission spectra went through three stages (see Fig. 4(a)–(c)). From 27 °C to 45 °C, the short wavelength edges of PBG were detected in Fig. 4(a). While from 46 °C to 55 °C, both the short and long wavelength edges of PBG were out of the spectrum range of BBS (see Fig. 4(b)). Further increasing the temperature

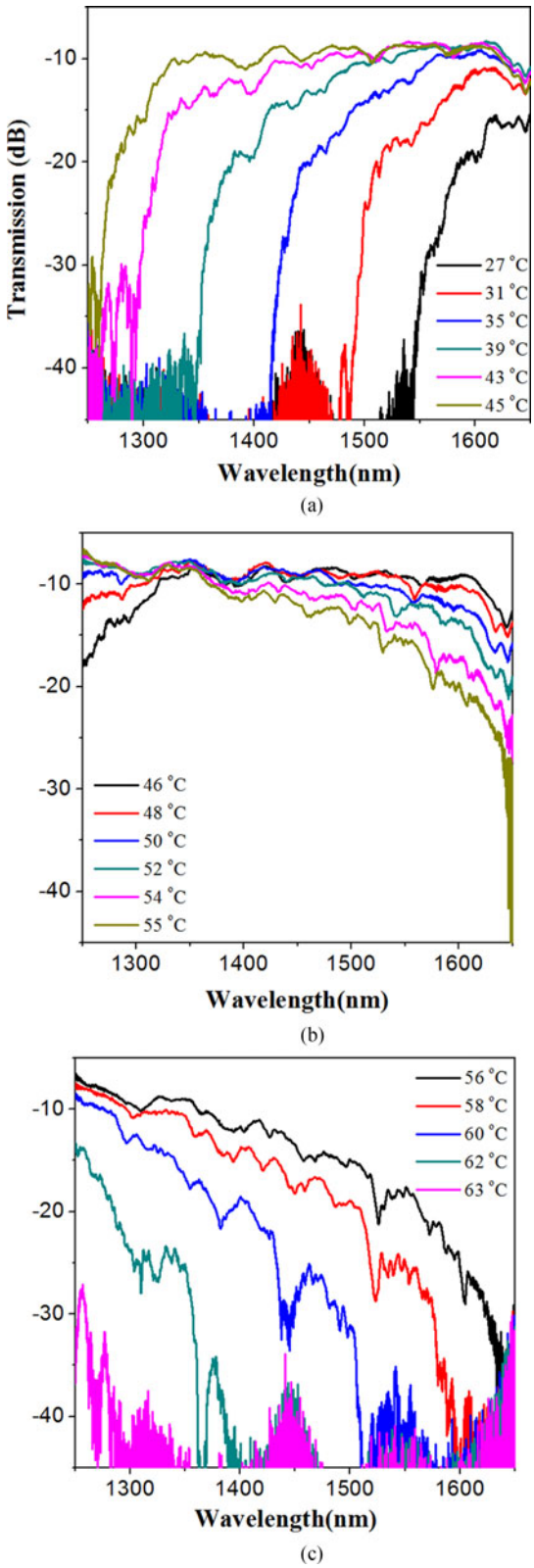

Fig. 4. Transmission spectra of the toluene-filled PM-PCF at temperature range (a) from 27 °C to 45 °C, (b) from 46 °C to 55 °C, and (c) from 56 °C to 63 °C.

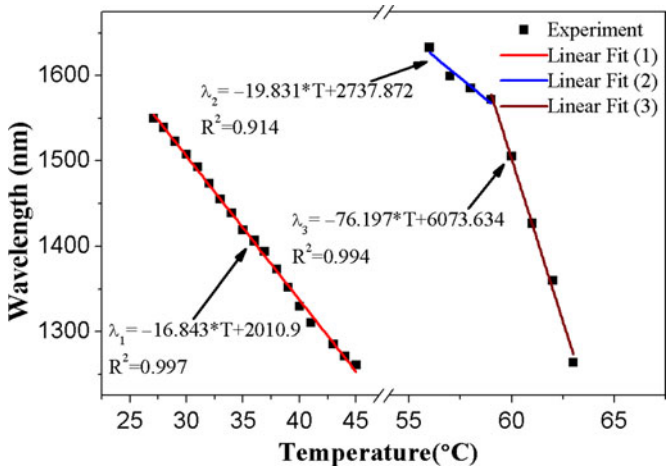

Fig. 5. Correlations between the wavelength of PBEs and temperature for the toluene-filled PM-PCF.

resulted in the only discovery of long wavelength edges from 56 °C to 63 °C (see Fig. 4(c)). In addition, the long wavelength edge shifted out of the spectrum range of BBS above 63 °C.

We also extracted the wavelengths corresponding to −35 dB, to quantitatively illustrate the wavelength shift of PBEs with temperatures (see Fig. 5). The temperature sensitivities are −16.843 nm/°C from 27 °C to 45 °C, −19.831 nm/°C from 56 °C to 59 °C, and −76.197 nm/°C from 59 °C to 63 °C, respectively. The temperature sensitivity of −76.197 nm/°C is higher than previously reported ones [15], [20]. According to the calculated results of bandgap, the high transmission window is always located in the first PBG of toluene-filled PM-PCF from 27 °C to 63 °C. The ultrahigh temperature sensitivity from 56 °C to 63 °C for the extracted PBEs are the long wavelength edges of first PBG, while the extracted PBEs from 27 °C to 45 °C are the short wavelength edges. That the temperature sensitivities increase with rising temperature is another reason of the ultrahigh sensitivity of ∼−76.197 nm/°C from 59 °C to 63 °C. Therefore, the high sensitivities of the toluene-filled PM-PCF on one hand originate from the high transmission window located in the first PBG and, on the other, are induced by the high thermo-optic coefficient of toluene.

5. Conclusion

In conclusion, we demonstrated a kind of compact structure and ultrasensitive temperature sensor using the liquid-filled PM-PCFs based on the MTIR and PBG guidance mechanism. In the glycerol-filled PM-PCF, the temperature sensitivity is up to −10.033 nm/°C from 38 °C to 45 °C. The high temperature sensitivities originate from the high transmission window located in the first PBG. Using a filler with higher thermo-optic coefficient (i.e., toluene), the temperature sensitivity increased to ∼−16.843 nm/°C from 27 °C to 45 °C, and remarkably to ∼−76.197 nm/°C from 59 °C to 63 °C. Therefore, higher temperature sensitivities can be expected with an optimization PCF structure and appropriate filler in further research. Furthermore, a wider range of testing temperature can be obtained by replacing the BBS with a broader spectrum. Both the PM-PCF and the liquid-filled PM-PCFs present unique birefringence properties, which will be investigated in our future work. The proposed structure and theoretical analysis in this paper also can apply for temperature sensing and tunable bandpass filters.

References

[1] J. C. Knight, “Photonic crystal fibers," *Nature*, vol. 424, no. 6950, pp. 847–851, Aug. 2003.
[2] P. Russell, “Photonic crystal fibers,” *Science*, vol. 299, no. 5605, pp. 358–362, Jan. 2003.

[3] Y. Liu *et al.*, "Compact tunable multibandpass filters based on liquid-filled photonic crystal fibers," *Opt. Lett.*, vol. 39, no. 7, pp. 2148–2151, Apr. 2014.
[4] B. Sun *et al.*, "Broadband thermo-optic switching effect based on liquid crystal infiltrated photonic crystal fibers," *IEEE Photon. J.*, vol. 7, no. 4, Aug. 2015, Art. no. 6802207.
[5] C. Kerbage *et al.*, "Integrated all-fiber variable attenuator based on hybrid microstructure fiber," *Appl. Phys. Lett.*, vol. 79, no. 19, pp. 3191–3193, Nov. 2001.
[6] B. Sun *et al.*, "Unique temperature dependence of selectively liquid-crystal-filled photonic crystal fibers," *IEEE Photon. Technol. Lett.*, vol. 28, no. 12, pp. 1282–1285, Jun. 2016.
[7] D. J. J. Hu *et al.*, "Fabrication and characterization of a highly temperature sensitive device based on nematic liquid crystal filled photonic crystal fiber," *IEEE Photon. J.*, vol. 4, no. 5, pp. 1248–1255, Oct. 2012.
[8] W. Yuan *et al.*, "Thermal tunability of photonic bandgaps in liquid crystal infiltrated microstructured polymer optical fibers," *Opt. Exp.*, vol. 17, no. 22, pp. 19356–19364, 2009.
[9] P. Zu *et al.*, "Magneto-optical fiber sensor based on bandgap effect of photonic crystal fiber infiltrated with magnetic fluid," *Appl. Phys. Lett.*, vol. 101, no. 24, Dec. 2012, Art. no. 241118.
[10] A. Candiani *et al.*, "A loss-based magnetic field sensor implemented in a ferrofluid infiltrated microstructured polymer optical fiber," *Appl. Phys. Lett.*, vol. 104, no. 11, 2014, Art. no. 111106.
[11] X. B. Zheng *et al.*, "Transmission and temperature sensing characteristics of a selectively liquid-filled photonic-bandgap-fiber-based Sagnac interferometer," *Appl. Phys. Lett.*, vol. 100, no. 14, Apr. 2012, Art. no. 141104.
[12] Y. Wang *et al.*, "Improved bending property of half-filled photonic crystal fiber," *Opt. Exp.*, vol. 18, no. 12, pp. 12197–12202, Jun. 2010.
[13] J. Du *et al.*, "Thermally tunable dual-core photonic bandgap fiber based on the infusion of a temperature-responsive liquid," *Opt. Exp.*, vol. 16, no. 6, pp. 4263–4269, Mar. 2008.
[14] S. J. Qiu *et al.*, "Temperature sensor based on an isopropanol-sealed photonic crystal fiber in-line interferometer with enhanced refractive index sensitivity," *Opt. Lett.*, vol. 37, no. 5, pp. 863–865, Mar. 2012.
[15] Y. Wang *et al.*, "Selectively infiltrated photonic crystal fiber with ultrahigh temperature sensitivity," *IEEE Photon. Technol. Lett.*, vol. 23, no. 20, pp. 1520–1522, Oct. 2011.
[16] Y. Peng *et al.*, "Temperature sensing using the bandgap-like effect in a selectively liquid-filled photonic crystal fiber," *Opt. Lett.*, vol. 38, no. 3, pp. 263–265, Feb. 2013.
[17] S. A. Cerqueira *et al.*, "Hybrid photonic crystal fiber," *Opt. Exp.*, vol. 14, pp. 926–931, 2006.
[18] L. Xiao, W. Jin, and M. S. Demokan, "Photonic crystal fibers confining light by both index-guiding and bandgap-guiding: Hybrid PCFs," *Opt. Exp.*, vol. 15, pp. 15637–15647, 2007.
[19] Y. Ould-Agha *et al.*, "Broadband bandgap guidance and mode filtering in radially hybrid photonic crystal fiber," *Opt. Exp.*, vol. 20, no. 6, pp. 6746–6760, Mar. 2014.
[20] T. Han *et al.*, "Control and design of fiber birefringence characteristics based on selective-filled hybrid photonic crystal fibers," *Opt. Exp.*, vol. 22, no. 12, pp. 15002–15016, Jun. 2014.
[21] N. M. Litchinitser *et al.*, "Resonances in microstuctured optical waveguides," *Opt. Exp.*, vol. 11, no. 10, pp. 1243–1251, May 2003.
[22] A. Samoc, "Dispersion of refractive properties of solvents: chloroform toluene benzene and carbon disulfide in ultraviolet visible and near-infrared," *J. Appl. Phys.*, vol. 94, pp. 6167–6174, 2003.
[23] Z. T. Cao *et al.*, "All-glass extrinsic Fabry-Perot interferometer thermo-optic coefficient sensor based on a capillary bridged two fiber ends," *Appl. Opt.*, vol. 54, pp. 2371–2375, Mar. 2015.